

# Interfacial fracture energy measurements for multi-walled carbon nanotubes pulled from a polymer matrix

Asa H. Barber <sup>a</sup>, Sidney R. Cohen <sup>b</sup>, Shmuel Kenig <sup>c</sup>, H. Daniel Wagner <sup>a,\*</sup>

<sup>a</sup> Department of Materials and Interfaces, Weizmann Institute of Science, Rehovot 76100, Israel

<sup>b</sup> Chemical Research Support, Weizmann Institute of Science, Rehovot 76100, Israel

<sup>c</sup> Department of Plastics Engineering, Shenkar College of Engineering and Design, Ramat-Gan 52526, Israel

Received 19 January 2004; accepted 26 January 2004

Available online 21 July 2004

## Abstract

Pullout experiments were performed at the nanoscale using an atomic force microscope, to assess the interfacial adhesion between multi-walled carbon nanotubes and a matrix of polyethylene–butene. Fracture energy for the nanotube–polymer interface was calculated from the measured pullout forces and embedded lengths. The results suggest the existence of a relatively strong interface, with higher fracture energy for smaller diameter nanotubes.

© 2004 Elsevier Ltd. All rights reserved.

*Keyword:* Nanotubes

## 1. Introduction

Carbon nanotubes can be considered as a potentially new class of reinforcement for polymer composites. A carbon nanotube is a cylindrical tubule containing sp<sup>2</sup> hybridized carbon–carbon bonds along its length. Both single-walled carbon nanotubes and the outer wall of multi-walled carbon nanotubes may be viewed as single molecules and, because of their nanosize, are potentially defect-free structures. Since the defect density in a fiber determines its mechanical properties [1], the scale advantage over current fibers such as glass or carbon is an understandable attraction. While recent studies have questioned whether the structure of carbon nanotubes is actually perfect [2], direct mechanical testing of individual nanotubes [3], as well as other indirect approaches such as Raman spectroscopy [4,5], fragmentation of nanotubes in a polymer due to compression [6–8], observation of nanotube freestanding vibrations [9] and computer simulation work [10,11],

indicate that properties such as Young's modulus, tensile strength and strain to failure are all in excess of those of conventional engineering fibers.

Efforts to produce carbon nanotube reinforced polymer composites initially showed disappointing results [12,13], probably due to poor dispersions of nanotubes within a polymer matrix. As better dispersions of nanotubes have been produced within the composites, such as through shear melt processing [14,15] or via chemical modification of the nanotube surface to improve dispersion [16], the mechanical properties of nanotube-based composites have improved dramatically.

The degree of interfacial adhesion between nanotubes and polymers is a key parameter in both the production and physical properties of carbon nanotube composites, and is important in understanding the surface behavior of nanoscale materials. Adequate interfacial stress transfer from the matrix to the reinforcement is only possible when the interface has not failed during composite loading. Failure of the interface effectively neutralizes the efficiency of the reinforcement. The structure of carbon nanotubes apparently shows little promise for forming a strong interface with a polymer matrix. A perfect sp<sup>2</sup> hybridized carbon structure has limited

\* Corresponding author. Tel.: +972-8-934-2594; fax: +972-8-934-4137.

E-mail address: [cpwagner@wis.weizmann.ac.il](mailto:cpwagner@wis.weizmann.ac.il) (H.D. Wagner).

ability to form any sort of strong covalent bonds with a surrounding polymer matrix. The atomically smooth nanotube surface is also poor for ‘mechanical interlocking’ effects that are known to improve fiber–matrix adhesion [17]. Weak van der Waals forces are the only a priori candidate for nanotube–polymer interaction. Computer simulations have shown that nanotube–polymer interactions can lead to strong interfacial strengths if certain criteria are met, such as wrapping of polymer matrix molecules around the nanotube [18,19] or introducing covalent bonding between the nanotube and polymer [20].

The work in our laboratory has shown, for the first time, that it is possible to detach a nanotube from a polymer matrix, either using a drag-out configuration [21] or a nano-pullout test [22]. The latter is analogous to the micromechanical single fiber pullout test. In particular, the nano-pullout test provides direct, reasonably reproducible measurements of the interfacial strength between a carbon nanotube and a polymer matrix and shows promise as a test to evaluate interfaces in nanocomposites. This paper expands on our previous work carried out using the single nanotube pullout method. We carry out single nanotube pullout experiments from a polymer matrix at small embedded lengths and evaluate the interfacial fracture energy.

## 2. Pullout theory

Single fiber pullout as a technique of measuring fiber–polymer adhesion has been in use for a number of years. The analysis of test data falls into two broad categories, namely stress-based or energy-based approaches. An energy-based analysis was preferred in the present work to quantify the pulling of a nanotube out of a polymer matrix. We base our approach mostly on the energy balance model of Jiang and Penn [23]. This scheme includes strain energy in the free fiber, strain energy stored in the debonded region, strain energy stored in the bonded region and a work of friction term. A crack is assumed to propagate at the interface between a fiber and a polymer matrix. As the interfacial crack propagates, the strain energy released from the system must supply the energy required to propagate an interfacial crack through the bonded interface region, as well as supply energy dissipated through friction in the previously debonded region

$$\frac{\partial U_{\text{fib}}}{\partial a} + \frac{\partial U_{\text{deb}}}{\partial a} + \frac{\partial U_{\text{bond}}}{\partial a} = 2\pi r G_c + \frac{\partial W_f}{\partial a}, \quad (1)$$

where  $U_{\text{fib}}$  is the total strain energy stored in the free fiber length,  $U_{\text{deb}}$  is the total strain energy stored in the debonded region,  $U_{\text{bond}}$  is the total strain energy stored in the bonded region,  $W_f$  is the work of friction at the debonded interface,  $r$  is the fiber radius and  $G_c$  is the

interfacial fracture energy. No initial crack corresponds to  $a = 0$ . Details of the calculations for the individual components can be found in reference [23]. By solving Eq. (1), the critical (maximum) force,  $F_c$ , at which the crack has fully propagated along the interface (while assuming small embedded lengths and negligible friction between the debonded fiber and polymer) can be used to give the interfacial fracture energy thus

$$F_c = \left(\frac{n}{r}\right) \ell \sqrt{\frac{E_f A_f 2\pi r G_c}{(2 + \alpha)}}, \quad (2)$$

where  $E_f$  is the fiber modulus,  $A_f$  is the cross-sectional fiber area,  $\alpha$  is equal to  $(E_f A_f)/(E_m A_m)$  ( $E_m$  and  $A_m$  are the matrix modulus and area respectively) and can be neglected because the matrix area ( $A_m$ ) is much larger than the nanotube area ( $A_f$ ),  $\ell$  is the embedded length and the constant  $n$ , a function of the matrix shrinkage around the fiber and a stress transfer parameter ( $R/r$ ), is given by

$$n = \sqrt{\frac{E_m}{E_f(1 + \nu_m) \ln(R/r)}}, \quad (3)$$

where  $\nu_m$  is the matrix Poisson’s ratio and  $R$  is the matrix radial distance from the fiber axis at which shear tends to zero. We have assumed that it is reasonable to extend the concepts and model above to nanoscale pullout experiments and Eq. (2) was used to evaluate the interfacial strength of nanotube–polymer specimens.

## 3. Experimental procedure

### 3.1. Sample preparation

Single multi-walled carbon nanotubes (MWCNTs, Nanolab, MA) were attached to AFM tips in the following way. MWCNT powder was used as provided and a small fraction (<0.01 g) was shaken onto carbon conducting tape. The carbon tape was then transferred to a scanning electron microscope (SEM, Philips XL300 ESEM). A nano-manipulator was used to position a single chip containing an AFM cantilever attached to the end of the manipulator arm within the SEM chamber under vacuum. By approaching isolated MWCNTs on the carbon tape, it was possible to pick up and attach a single MWCNT to the AFM tip. Moving the AFM tip into bundles of MWCNTs and then removing could also cause isolated nanotubes to adhere to the end of the AFM tip through van der Waals interactions between the AFM tip and the tubes themselves.

To further secure each single MWCNT to the AFM tip, amorphous carbon deposition at the base of the nanotube was performed as described in previous work [24]. The deposition was performed at typical SEM acceleration voltages of 20 kV for 15 min while focusing

on the part of the nanotube attached to the apex of the AFM tip using magnifications approaching  $1,000,000\times$ . This method of affixing nanotubes to AFM tips was previously shown to produce extremely robust scanning probes [24]. Care was taken not to image the free nanotube length during all SEM investigations as the SEM electron beam might possibly cause damage or further amorphous carbon deposition onto the free nanotube length. An example of an attached carbon nanotube to an AFM tip is given in Fig. 1.

A thin film of a low melting temperature thermoplastic of polyethylene–butene (ExxonMobil Research and Engineering, USA) was spin coated onto a sapphire plate from a decalin solution, and allowed to dry under vacuum for 72 h. Using solutions containing 10% by weight of polyethylene–butene, the resultant films were approximately 300 nm thick. A typical stress–strain curve for a bulk specimen is given in Fig. 2. The Young's

modulus of this polymer is approximately 10 MPa and the strength to break is 8 MPa.

### 3.2. Pullout testing

The polymer film was heated *in situ* on an AFM (NT-MDT Solver P47, Zelenograd) up to approximately  $50\text{ }^{\circ}\text{C}$ . From imaging the polymer surface during heating, the polyethylene–butene appeared to start flowing in a liquid-like manner at  $38\text{ }^{\circ}\text{C}$ . Once the polymer film was at the peak temperature, the AFM–nanotube tip was lowered towards the molten polymer surface. On contact with the polymer film, the nanotube tip experienced a small jump into the polymer of about 10 nm, probably corresponding to wetting effects between the polymer and the nanotube. The AFM could then be used to push the nanotube further into the molten polymer. This process was restricted, as excessive push of the nanotube within the polymer would often cause the nanotube to bend as it moved through the viscous fluid, due to the high aspect ratio of the nanotube. This could be alleviated to some extent by using smaller aspect ratio nanotubes on the AFM tip i.e. increased nanotube diameter or reduced nanotube free length. Once embedded within the polymer, the film was allowed to air-cool to just above room temperature while the AFM feedback maintained the nanotube position within the polymer. The nanotube tip was then retracted from the solid polymer and the cantilever deflection monitored during this process with a digital scope (Nicolet 300) so that the force profile during the nano-pullout could be measured. Finally, the pullout area on the solid polymer surface was imaged using the pulled-out nanotube–AFM tip. The pullout depth was taken from these AFM topography images. To check if this depth was accurate and if the imaging nanotube–AFM tip could penetrate to the bottom of the hole, a small number of experiments were conducted where the embedded length of the nanotube within the liquid polymer was calculated from changes in the z-piezo and cantilever deflection during the jump-in/push-in of the nanotube into the liquid polymer. This technique showed good agreement with the measured embedded lengths from the AFM topography images. Nano-pullout experiments were repeated with many nanotube–AFM tips of varying nanotube diameter. After every pullout, each nanotube tip was examined using high resolution SEM and every tube retained its free length and diameter, indicating that the pullout was ‘clean’ and that nanotube fracture had not occurred.

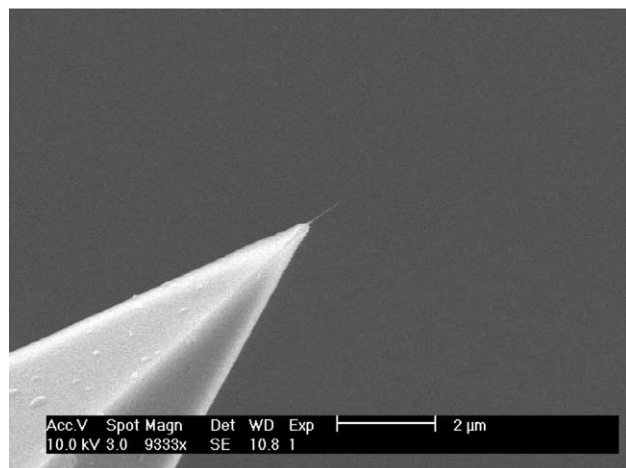


Fig. 1. High resolution SEM picture of a single MWCNT on a silicon AFM tip.

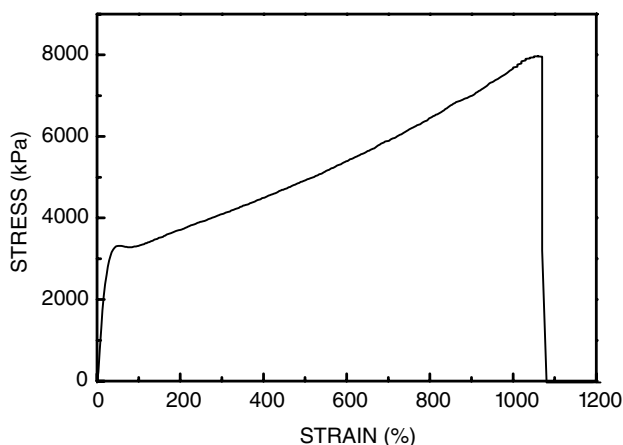


Fig. 2. Typical stress–strain curve for a sample of polyethylene–butene.

## 4. Results

The polymer was imaged both before and after nanotube pullout. A typical pullout hole is shown in

Fig. 3. A number of pullout tests were performed and the maximum pullout force was collected by monitoring the cantilever deflection during each test. This deflection signal was converted into a pullout force by first contacting the AFM tip with a hard surface and measuring the cantilever deflection signal change while performing a force distance curve using the AFM. This gives the deflection signal in terms of cantilever deflection distance. The geometry of each cantilever was then measured using a high resolution SEM and the resultant spring constant,  $k$ , calculated using

$$k = \frac{Ebt^3}{4L^3}, \quad (4)$$

where  $E$  is the Young's modulus of the silicon cantilever (taken as 170 GPa [25]), and  $b$ ,  $L$  and  $t$  are the breadth (width), length and thickness of the cantilever, respectively. The value of the cantilever spring constant can then be used to calculate the maximum force from the cantilever deflection signal during nanotube pullout. An example of a plot of the pullout force against embedded nanotube length within the polymer is shown in Fig. 4.

To evaluate the fracture energy of the nanotube–polymer interface, Eq. (2) is rearranged to give

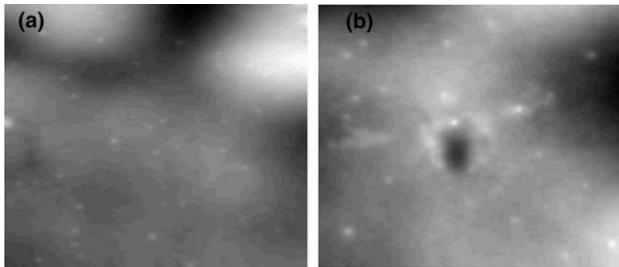


Fig. 3. AFM topography image of polyethylene-butene (a) at room temperature before testing and (b) after the pullout experiment. Note: the horizontal scan size was 1  $\mu\text{m}$ .

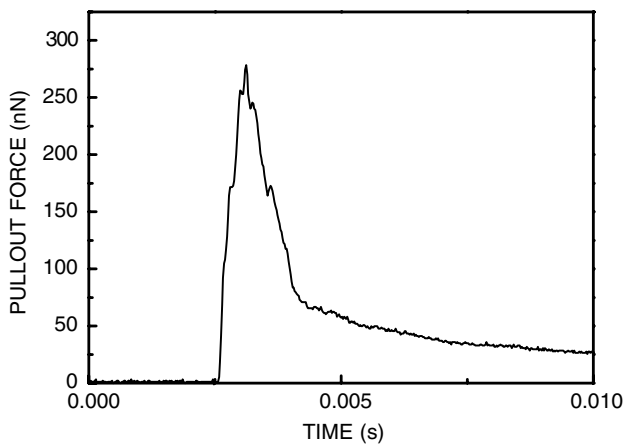


Fig. 4. Pullout curve measured during retraction of a single MWCNT embedded within a matrix of polyethylene-butene.

$$F_c = \left( \frac{Kn}{r} \right) \ell \sqrt{G_c}, \quad (5)$$

where  $K$  is a constant dependent on the nanotube geometry such that

$$K = \sqrt{E_t A_t \pi r}. \quad (6)$$

By plotting the maximum pullout force,  $F_c$ , against the embedded length of the nanotube within the polymer,  $\ell$ , one is able to calculate the interfacial fracture energy  $G_c$  using Eq. (5). One complication arises when applying Eq. (5) since the nanotube diameter is variable. This can be overcome by collecting specimens with similar nanotube radii into groups, as shown in Fig. 5. The nanotube radii were grouped into the following ranges: 10–20, 30–40, 40–50 and 60–70 nm. On Fig. 5 the average gradient values ( $\delta F_c / \delta \ell$ ) for each grouping was used to calculate the interfacial fracture energy  $G_c$ . A final issue concerns the constant  $n$ , which contains the stress transfer parameter  $R/r$ . This parameter is used to describe the mean average spacing between fiber reinforcements in anisotropic composite materials. In the nanotube pullout configuration studied here the  $R/r$  parameter cannot be determined. In Fig. 6,  $G_c$  is plotted against representative  $R/r$  values for each nanotube grouping. The  $R/r$  range is limited to typical composite values: generally around 2–3 for weak composite interfacial strengths or up to 9 for strong interfaces [26,27]. As seen in Fig. 6, the pullout energy varies from around 4–70  $\text{J m}^{-2}$ . A plot of the interfacial shear strength,  $\tau$  against nanotube radius is presented in Fig. 7. This was calculated by simply dividing the pullout force by the lateral area  $2\pi r \ell$ .

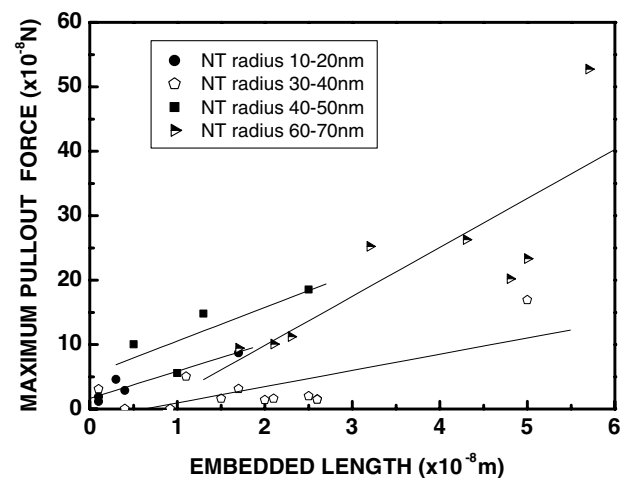


Fig. 5. Plot of maximum force,  $F_c$ , required to pull a nanotube of embedded length  $\ell$  from polyethylene-butene for nanotubes of different radii. The different nanotube diameter groupings are highlighted with different symbols. A best fit line, used to calculate  $\Delta F_c / \delta \ell$ , is fitted through different nanotube diameter groupings are highlighted with different symbols as well as a best fit line, used to calculate each nanotube diameter grouping.

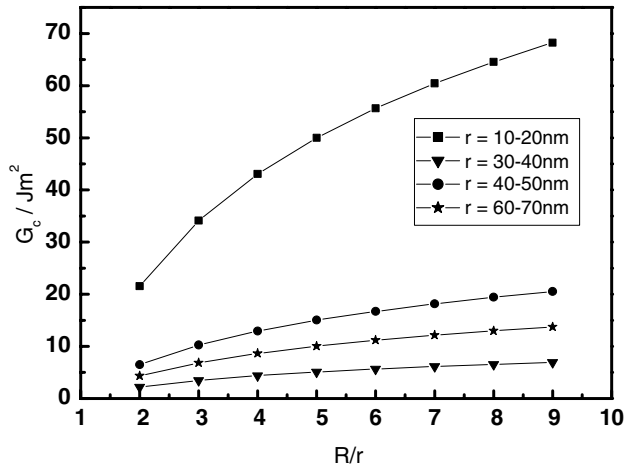


Fig. 6. Plot of the calculated interfacial fracture energy for the pullout of a single MWCNT from a polyethylene-butene matrix for differing  $R/r$  values.

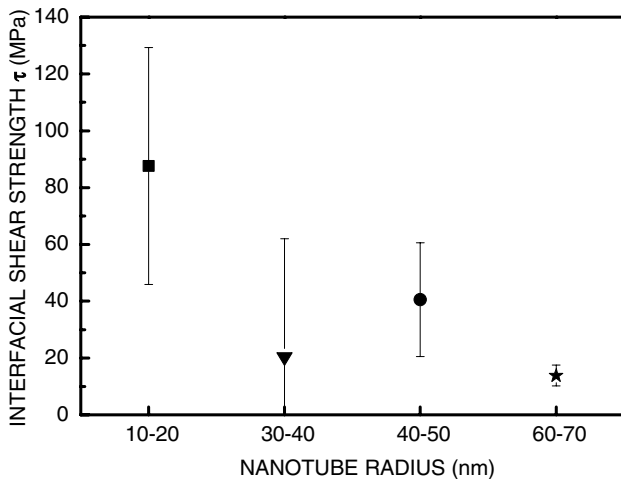


Fig. 7. Plot of the interfacial shear strength against nanotube radius ranges.

## 5. Discussion

A characteristic plot of the pullout of a nanotube from a polymer is displayed in Fig. 4. This plot is similar to typical pullout plots for conventional micron-sized fibers in polymer matrices. The pullout of the nanotube from the surrounding matrix first involves an increase in the pullout force while the nanotube remains in full contact with the polymer. As the force increases on the nanotube, both the interfacial shear force and the tensile force at the nanotube end increase. Further displacement of the nanotube away from the polymer causes initiation and growth of a debonded region until, at a critical maximum force, the nanotube fully debonds from the polymer matrix. This full debonding is followed by a sharp drop in the recorded force due to a fully failed interface. SEM micrographs of the pulled out

nanotubes show no evidence of polymer residues on the nanotube surface, indicating that the nanotube-polymer failure occurred at the nanotube-polymer boundary and not within the polymer matrix. Further displacement of the nanotube occurs, with the only forces acting on the tube after full debonding being due to frictional interactions. For the small embedded lengths used within this work, the frictional interaction is minimal as the force drops rapidly from the maximum pullout force to quasi-zero force acting on the tube. In traditional fiber composites, the drop in force from the maximum pullout force is usually followed by a pullout 'shoulder', not seen here, which reflects the force required to overcome the frictional interaction between fiber and polymer matrix. As carbon nanotubes are atomically smooth, it is reasonable to assume that the nanotube slides out relatively easily from the surrounding polymer matrix after full nanotube debonding from the matrix. Similarly, other experiments carried out previously in our laboratory using a drag-out technique with larger embedded nanotube lengths within an epoxy matrix [21] showed no evidence of a pullout 'shoulder'.

The present nanotube pullout tests show that the range of interfacial fracture energies required to remove a nanotube from a thermoplastic polymer matrix, between 4 and 70  $\text{J m}^{-2}$ , is comparable to that of fiber pullout in other engineering composite systems. For example, a recent study [28] gave a range of interfacial fracture energy values for glass fibers pulled from a variety of polymers such as maleic anhydride modified polypropylene (6–7  $\text{J m}^{-2}$ ), vinyl ester (13–34  $\text{J m}^{-2}$ ), polyamide 6 (24–93  $\text{J m}^{-2}$ ) and polyamide 6.6 (52–61  $\text{J m}^{-2}$ ). These fibers were chemically modified to induce strong bonding between the matrix and reinforcement. The differences in the interfacial fracture energy between nanotube-polymer and fiber-polymer systems may be attributed to a number of phenomena. We already showed that the overall energy required to separate a nanotube from a polymer does not contain major contributions from frictional forces between the nanotube and polymer matrix. The smooth nanotube outer surfaces also cause the calculated contact area with the polymer to be rather precise whereas larger, rougher surfaces in fibers result in an under-estimation of the fiber surface area for typical engineering reinforcements (since the average fiber diameter is used in the calculation), leading to an over-estimation of the actual interfacial fracture energy. It is in fact remarkable that the level of interfacial energies measured here in carbon nanotube-polymer matrix composites compare rather well with the interfacial energies observed in systems with strong interfacial bonding. This may suggest that the carbon nanotubes in this study interact with the surrounding polymer matrix not just by van der Waals interactions but possibly through bonding with the polymer via defects in the nanotube structure or perhaps

due to polymer chains wrapping round the nanotube itself. In particular, the nanotubes from the smallest radii groupings show significantly higher interfacial fracture energies (Fig. 6) when compared with the other nanotube groupings. This may reflect the existence of a nanotube size effect on the interfacial fracture energy, with smaller nanotube diameters forming stronger interfaces with the polymer matrix than larger nanotube diameters. The same conclusion may be reached from an examination of the interfacial shear strength on Fig. 7, although end effects may play a significant role too because the embedded lengths in this work are rather short.

The different interfacial energies (or interfacial strengths) observed for thinner and thicker nanotubes may be attributed to surface differences, with thinner nanotubes possibly having a smaller radius of curvature compared with the thicker diameter nanotubes, thus a higher strain energy leading to a larger number of defects with which to form bonds with the polymer matrix.

## 6. Conclusions

Pullout tests of MWCNTs from a polyethylene-butene matrix were performed using an AFM-based technique developed in our laboratory. The maximum pullout force and embedded length were used to estimate the total interfacial fracture energy for the pullout process. The results suggest the existence of a relatively strong interface, with higher fracture energy for smaller diameter nanotubes. The interfacial fracture energy level is comparable to that in composite systems possessing strong interfaces. The results presented here suggest that tougher composites may result from the increased interfacial fracture energies observed when nanotubes are used as a reinforcing phase.

## Acknowledgements

This project was supported by the (CNT) Thematic European network on “Carbon Nanotubes for Future Industrial Composites” (EU), the Minerva Foundation, the G.M.J. Schmidt Minerva Centre of Supramolecular Architectures, and by the Israeli Academy of Science. H.D. Wagner is the incumbent of the Livio Norzi Professorial Chair, and wishes to acknowledge the inspiring assistance of B. Goodman and L. Hampton.

## References

- [1] Weibull W. A statistical distribution function of wide applicability. *J Appl Mech* 1951;18:293–7.
- [2] Zhou LG, Shi SQ. Adsorption of foreign atoms on Stone–Wales defects in carbon nanotube. *Carbon* 2003;41:613–5.
- [3] Wong EW, Sheehan PE, Lieber CM. Nanobeam mechanics: elasticity, strength and toughness of nanorods and nanotubes. *Science* 1997;277:1971–5.
- [4] Zhao Q, Frogley MD, Wagner HD. The use of carbon nanotubes to sense matrix stresses around a single glass fiber. *Compos Sci Technol* 2001;61(14):2139–43.
- [5] Cooper CA, Young RJ, Halsall M. Investigation into the deformation of carbon nanotubes and their composites through the use of Raman spectroscopy. *Composites A* 2001;32(3–4):401–11.
- [6] Lourie O, Wagner HD. Evidence of stress transfer and formation of fracture clusters in carbon nanotube-based composites. *Compos Sci Technol* 1999;59(6):975–7.
- [7] Lourie O, Cox DM, Wagner HD. Buckling and collapse of embedded carbon nanotubes. *Phys Rev Lett* 1998;81(8):1638–41.
- [8] Wagner HD, Lourie O, Feldman Y, Tenne R. Stress-induced fragmentation of multiwall carbon nanotubes in a polymer matrix. *Appl Phys Lett* 1998;72(2):188–90.
- [9] Krishnan A, Dujardin E, Ebbesen TW, Yianilos PN, Treacy MMJ. Young’s modulus of single-walled nanotubes. *Phys Rev B* 1998;58:14013–9.
- [10] Yakobson BI, Campbell MP, Brabec CJ, Bernolc J. High strain rate fracture of C-chain unraveling in carbon nanotubes. *Compos Mater Sci* 1997;8:341–8.
- [11] Lu JP. Elastic properties of carbon nanotubes and nanoropes. *Phys Rev Lett* 1997;79(7):1297–300.
- [12] Ajayan PM, Schadler LS, Giannaris C, Rubio A. Single-walled carbon nanotube-polymer composites: strengths and weakness. *Adv Mater* 2000;12(10):750–3.
- [13] Schadler LS, Giannaris C, Ajayan PM. Load transfer in carbon nanotube epoxy composites. *Appl Phys Lett* 1998;73(26):3842–4.
- [14] Kearns JC, Shambaugh RL. Polypropylene fibers reinforced with carbon nanotubes. *J Appl Poly Sci* 2002;86:2079–84.
- [15] Thorstenson ET, Chou T-W. Aligned multi-walled carbon nanotube-reinforced composites: processing and mechanical characterization. *J Phys D: Appl Phys* 2002;35:L77–80.
- [16] Sinnott SB. Chemical functionalization of carbon nanotubes. *J Nanosci Nanotechnol* 2002;2(2):113–23.
- [17] Hull D. An introduction to composite materials. second ed. Cambridge: Cambridge University Press; 1996.
- [18] Lordi V, Yao N. Molecular mechanics of binding in carbon-nanotube-polymer composites. *J Mater Res* 2000;15(12):2770–9.
- [19] in het Panhuis M, Maiti A, Dalton AB, vander Noort A, Coleman JN, McCarthy B, et al. Selective interactions in a polymer-single-wall carbon nanotube composite. *J Phys Chem B* 2003;107:478–82.
- [20] Frankland SJV, Caglar A, Brenner DW, Griebel M. Molecular simulations of the influence of chemical cross-links on the shear strength of carbon nanotube-polymer interfaces. *J Phys Chem B* 2002;106:3046–8.
- [21] Cooper CA, Cohen SR, Barber AH, Wagner HD. Detachment of nanotubes from a polymer matrix. *Appl Phys Lett* 2002;81(20):3873–5.
- [22] Barber AH, Cohen SR, Wagner HD. Measurement of carbon nanotube-polymer interfacial strength. *Appl Phys Lett* 2003;82(23):4140–2.
- [23] Jiang KR, Penn LS. Improved analysis and experimental evaluation of the single filament pull-out test. *Compos Sci Technol* 1992;45:89–103.
- [24] Nishijima H, Kamo S, Akita S, Nakayama Y, Hohmura KI, Yoshimura SH, et al. Carbon-nanotube tips for scanning probe microscopy: Preparation by a controlled process and observation of deoxyribonucleic acid. *Appl Phys Lett* 1999;74(26):4061–3.

- [25] Liu Y, Wu T, Evans DF. Lateral force microscopy study on the shear properties of self-assembled monolayers of dialkylammonium surfactant on mica. *Langmuir* 1994;10: 2241–5.
- [26] Galiotis C. Interfacial studies on model composites by laser Raman spectroscopy. *Compos Sci Technol* 1991;42(1–3):125–50.
- [27] Detassis M, Frydman E, Vrieling D, Zhou XF, Wagner HD, Nairn JA. Interface toughness in fibre composites by the fragmentation test. *Composites A* 1996;27(9):769–73.
- [28] Zhandarov S, Pisanova E, Mader E, Nairn JA. Investigation of load transfer between the fiber and the matrix in pull-out tests with fibers having different diameters. *J Adh Sci Technol* 2001;15(2):205–22.